Journal of Hydrology 558 (2018) 532–545

Contents lists available at ScienceDirect

Journal of Hydrology

journal homepage: www.elsevier.com/locate/jhydrol

Research papers

A field evaluation of soil moisture modelling with the Soil, Vegetation, and Snow (SVS) land surface model using evapotranspiration observations as forcing data

Audrey Maheu [a,*], François Anctil [b], Étienne Gaborit [c], Vincent Fortin [c], Daniel F. Nadeau [b], René Therrien [d]

[a] Département des sciences naturelles, Université du Québec en Outaouais, Canada
[b] Département de génie civil et de génie des eaux, Université Laval, Canada
[c] Environment and Climate Change Canada, Canada
[d] Département de géologie et de génie géologique, Université Laval, Canada

ARTICLE INFO

Article history:
Received 2 October 2017
Received in revised form 26 January 2018
Accepted 31 January 2018
Available online 2 February 2018
This manuscript was handled by P. Kitanidis, Editor-in-Chief, with the assistance of J. Simunek, Associate Editor

Keywords:
Soil moisture
Land surface model
SVS
HydroGeoSphere

ABSTRACT

To address certain limitations with their current operational model, Environment and Climate Change Canada recently developed the Soil, Vegetation, and Snow (SVS) land surface model and the representation of subsurface hydrological processes was targeted as an area for improvement. The objective of this study is to evaluate the ability of HydroSVS, the component of SVS responsible for the vertical redistribution of water, to simulate soil moisture under snow-free conditions when using flux-tower observations of evapotranspiration as forcing data. We assessed (1) model fidelity by comparing soil moisture modelled with HydroSVS to point-scale measurements of volumetric soil water content and (2) model complexity by comparing the performance of HydroSVS to that of HydroGeoSphere, a state-of-the-art integrated surface and subsurface hydrologic model. To do this, we performed one-dimensional soil column simulations at four sites of the AmeriFlux network. Results indicate that under Mediterranean and temperate climates, HydroSVS satisfactorily simulated soil moisture (Nash-Sutcliffe efficiency between 0.26 and 0.70; $R^2 \geq 0.80$), with a performance comparable to HydroGeoSphere (Nash-Sutcliffe efficiency $\geq$0.60; $R^2 \geq 0.80$). However, HydroSVS performed weakly under a semiarid climate while HydroGeoSphere performed relatively well. By decoupling the magnitude and sourcing of evapotranspiration, this study proposes a powerful diagnostic tool to evaluate the representation of subsurface hydrological processes in land surface models. Overall, this study highlights the potential of SVS for hydrological applications.

Crown Copyright © 2018 Published by Elsevier B.V. All rights reserved.

1. Introduction

Land surface models describe the interactions between the atmosphere and the land surface by simulating exchanges of momentum, heat and water within the Earth system. Land surface models provide the bottom boundary conditions for atmospheric models and are a key element of numerical weather prediction systems and climate change projection modelling. The ability of land surface models to capture hydrological processes is crucial to represent land-atmosphere coupling (Clark et al., 2015a; Maxwell et al., 2007). Subsurface hydrological processes are particularly important for modelling land-atmosphere interactions because soil moisture plays a key role in modulating fluxes and stores of water and energy. Indeed, soil moisture reflects precipitation storage, constrains evapotranspiration under water-limiting conditions and influences the partitioning of precipitation into infiltration and runoff (Seneviratne et al., 2010).

Despite their importance for land-atmosphere coupling, subsurface hydrological processes have typically been represented in a simplified form in many land surface models (Clark et al., 2015a; Davison et al., 2016). In particular, operational land surface models geared towards weather forecasting tend to simplify the representation of hydrological processes to minimize computational costs. Environment and Climate Change Canada currently uses a modified version of the Interactions between Soil, Biosphere, and Atmosphere (ISBA) land surface model to produce operational weather forecasts. Accordingly, the ISBA model provides surface fluxes of momentum, water, and energy to the Global Environmental Multiscale (GEM) atmospheric model. In ISBA, soil moisture is modelled using a force-restore approach involving only two soil layers extending to the assumed root depth (Bélair et al., 2003).

* Corresponding author.
E-mail address: audrey.maheu@uqo.ca (A. Maheu).

https://doi.org/10.1016/j.jhydrol.2018.01.065
0022-1694/Crown Copyright © 2018 Published by Elsevier B.V. All rights reserved.

To address certain limitations with ISBA, Environment and Climate Change Canada developed the Soil, Vegetation, and Snow (SVS) land surface model, with the representation of subsurface hydrological processes targeted as an area for improvement. In the hydrological module of SVS, HydroSVS, the soil column is now represented with increased vertical resolution and the vertical movement of water through the soil is now described using a finite difference solution of Richards' equation for unsaturated flow (Alavi et al., 2016). Two studies recently compared the performance of SVS and ISBA in offline mode and found that modifications implemented in SVS improved the simulation of soil moisture and brightness temperature during the warm season over the North American domain (Alavi et al., 2016; Husain et al., 2016). With these improvements, SVS coupled with a routing scheme now offers a computationally efficient tool for hydrological prediction. For example, SVS coupled to the WATROUTE routing scheme yielded a runoff simulation performance similar to two widely used distributed hydrological models, MESH and WATFLOOD, for the Lake Ontario watershed (Gaborit et al., 2017). Moreover, land surface models also offer a tool for hydrologists to better integrate land-atmosphere interactions in hydrological modelling (see for instance Maxwell et al., 2007; Soulis et al., 2000; Zabel and Mauser, 2013).

Various model evaluation and comparison initiatives have been undertaken in the land surface modelling community and have fuelled their rapid evolution (Henderson-Sellers et al., 1995, 1993; Van Den Hurk et al., 2011). While two studies have recently evaluated the global performance of SVS at the continental scale (Alavi et al., 2016; Husain et al., 2016), relevant diagnostics that can pinpoint problematic parameterization of processes are also needed. For example, point-scale assessments are essential to answer questions regarding the ability of a model to capture the temporal and spatial variability of certain variables such as soil moisture. An efficient evaluation of model fidelity in reproducing observations often relies on the isolation of individual processes (Clark et al., 2015b). As such, in the present study, subsurface hydrological processes (infiltration, percolation, vegetation water uptake) are specifically targeted. While most studies generally focus on evaluating model fidelity (e.g. the ability of the model to reproduce observations), a joint evaluation of model fidelity and complexity facilitates a clear assessment of trade-offs between different modelling options. For instance, potential performance gains associated with increased complexity can be evaluated in light of their added computational cost.

Building upon previous evaluations of SVS at a continental scale, the objective of the present study is to evaluate the representation of subsurface hydrological processes in HydroSVS. This study focuses on the performance of HydroSVS at the point-scale over a multiyear horizon. To do so, we follow an evaluation framework that (1) isolates subsurface hydrological processes by targeting study sites that are part of the AmeriFlux network where measured surface fluxes such as evapotranspiration can be used as forcing data; (2) evaluates model fidelity by comparing soil moisture modelled with HydroSVS to point-scale measurements at various depths and 3) assesses model complexity by comparing the soil moisture modelling performance of HydroSVS to HydroGeoSphere, a state-of-the art integrated surface and subsurface hydrologic model.

2. Study area

2.1. Description of AmeriFlux sites

We selected four study sites from the AmeriFlux network (Baldocchi et al., 2001) where surface fluxes were measured using the eddy-covariance method (Fig. 1). AmeriFlux sites are all subject to a series of data harmonization and quality control measures that facilitate site intercomparison. The following criteria were used for site selection: (1) volumetric soil water content measurements available at multiple depths and for multiple years, (2) absence of snow cover to specifically target warm-season subsurface hydrological processes and (3) representation of contrasting climates and vegetation types. Table 1 describes the four study sites and their associated climates (semiarid, Mediterranean, temperate) and vegetation types (grassland, woody savanna, deciduous broadleaf forest, evergreen needleleaf forest). In terms of climate and seasonality, a semiarid climate prevails at US-Wkg and 60% of the annual precipitation occurs during the North American monsoon in July, August, and September (Moran et al., 2009a; Scott et al., 2010). The US-Ton site is characterized by a Mediterranean climate and precipitation largely occurs during the winter months (October to May) with very little rainfall during the summer. The US-MRf site also has a Mediterranean climate with a relatively dry summer but precipitation during the wet winter months is about three times greater than at US-Ton. The US-WBW site has a temperate climate with a year-round supply of precipitation.

Precipitation and water vapor flux data at a 30-min time step were extracted from the AmeriFlux database (http://ameriflux.lbl.gov/; Baldocchi et al., 2001). Soil moisture data were extracted from the CDIAC-hosted database (Carbon Dioxide Information Analysis Center, http://cdiac.esd.ornl.gov/programs/ameriflux/data_system/aamer.html), given that observations were available at multiple depths (unlike the typical two measurement levels found in the AmeriFlux database). Across the study sites, soil moisture was measured with a variety of probes that generally derive volumetric soil water content by measuring an electrical property of the soil. More specifically, Theta ML2-X probes (Delta-T Devices) were deployed at US-Ton and US-WBW (Miller et al., 2007), Stevens Water Hydra Probe sensors at US-Wkg (Keefer et al., 2008), and Campbell Scientific CS615 probes at US-MRf (Kwon et al., 2017). Measurement accuracy typically ranges between 0.01 and 0.05 $m^3\ m^{-3}$ for the sensors used.

3. Methodology

3.1. Description of the SVS model

A detailed description of HydroSVS, the hydrology scheme of SVS, can be found in Alavi et al. (2016). In HydroSVS, the vertical

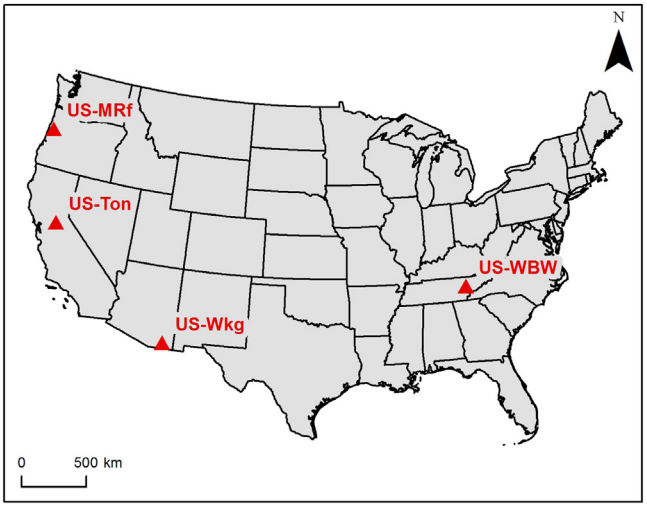

Fig. 1. Location of the four AmeriFlux study sites.

Table 1
Description of the four study sites.

	US-Wkg	US-Ton	US-MRf	US-WBW
Latitude/longitude	31.737, −109.942	38.432, −120.966	44.646, −123.551	35.959, −84.287
Elevation (m)	1531	177	263	283
Climate	Semiarid	Mediterranean	Mediterranean	Temperate
Koppen climate class	BSk: steppe, warm winter	Csa: Mediterranean, mild with dry, hot summer	Csb: Mediterranean, mild with dry, warm summer	Cfa: humid subtropical, mild with no dry season, hot summer
IGPB vegetation class	Grassland	Woody savanna	Evergreen needleleaf forest	Deciduous broadleaf forest
Soil type	Sandy loam[†]	Silt loam[¶]	Silty clay loam[¥]	Silt loam[¶]
Mean annual precipitation (mm)	407	559	1820	1372
Mean annual temperature (°C)	15.6	15.8	10.2	13.7
data source	Scott (2016)	Baldocchi (2016)	Law (2016)	Meyers (2016)

[†] Nearing et al. (2005).
[¶] Miller et al. (2007).
[¥] Biological, Ancillary, Disturbance and Metadata (BADM) from the AmeriFlux network.

movement of water is described by the one-dimensional Richards equation for unsaturated flow in a porous medium (Soulis et al., 2000). The evolution of moisture in soil layers is described using the conservation equation:

$$\frac{\partial\theta}{\partial t} = \frac{\partial F}{\partial z} + S \tag{1}$$

where θ is the volumetric soil water content ($m^3\ m^{-3}$), F is the water flux (kg $m^{-2}\ s^{-1}$), and S is the sink-source term (kg $m^{-2}\ s^{-1}$) that includes precipitation, evapotranspiration, surface runoff, lateral flow, base flow (at the bottom of the soil layer) as well as snow runoff, melting and freezing. The water flux $F(z,t)$ at depth z and time t is described by Darcy's law:

$$F(z,t) = K_v(z,t)\left(\frac{\partial\psi}{\partial z} + 1\right) \tag{2}$$

where $K_v(z,t)$ is the vertical hydraulic conductivity (m s^{-1}) and $\psi(z,t)$ is the soil water potential (m).

In HydroSVS, Eq. (1) is solved numerically using a fourth order Runge-Kutta finite difference method. The soil column is discretized into soil layers, whose depth and exact number can be defined by the user, and the water flux between each layer can be computed with Darcy's law. The relationship between soil water content, soil water potential and relative permeability follows the Clapp and Hornberger (1978) model.

Among sink and source terms, the evaporation and transpiration fluxes are typically derived from the SVS simulation of the energy budget using a force-restore approach (Husain et al., 2016). Accordingly, each grid cell is divided into the three surface types found in the model (bare ground, low vegetation and high vegetation) and a distinct energy budget is computed for each surface type. Instead, in this study, we used the eddy covariance-measured water vapor flux as a forcing to the model (see Section 3.4 for a description of the boundary conditions). With the exception of the semiarid site (US-Wkg), we assumed a land cover consisting exclusively of high vegetation. In the absence of information on evapotranspiration partitioning into evaporation (soil and wet canopy) and transpiration, we assumed that, at these sites (US-Ton, US-MRf, US-WBW), the surface water vapor flux occurred exclusively through transpiration. As such, soil evaporation and interception were considered negligible. At the semiarid site (US-Wkg) where vegetation is sparse and transpiration accounts for 79% of evapotranspiration during the monsoon period (Moran et al., 2009b), we assumed land cover was made up of bare soil at 25% and low vegetation at 75%. Accordingly, bare soil evaporation (i.e. 25% of the observed evapotranspiration used as forcing) was removed from the top soil layer and the remaining flux occurred through transpiration as it is the case for the three other sites. At all sites, water uptake from transpiration was distributed over the soil column as a function of the root profile and transpiration reduction function:

$$T(z) = ET_{obs}\, r(z) f(\theta) \tag{3}$$

where $T(z)$ is the evapotranspiration rate (kg $m^{-2}\ s^{-1}$) at depth z (m), ET_{obs} is observed evapotranspiration (kg $m^{-2}\ s^{-1}$), as measured at the flux tower, $r(z)$ is the root distribution function and $f(\theta)$ is the transpiration reduction function. The proportion of roots in a soil layer n corresponds to:

$$r(z) = r(z_n) - r(z_{n-1}) \tag{4}$$

where $r(z_n)$ is the fraction of roots above the soil layer depth z_n (m) and is described using the equation proposed by Schenk and Jackson (2003):

$$r(z_n) = \frac{1}{1 + (z_n/z_{50})^c} \tag{5}$$

where z_{50} is the depth (m) above which 50% of roots are found and c is a shape parameter. z_{50} was set to about 40% of the maximum root depth (0.5 m at US-Wkg; 0.3 m at US-Ton; 1 m at US-MRf; 0.25 at US-WBW). The shape parameter c was derived from z_{50} and the maximum root depth (see Husain et al., 2016).

The transpiration reduction function was parameterized as a step function given that observed (rather than potential) evapotranspiration was provided as a forcing:

$$f(\theta) = \begin{cases} 0 & \text{for } \theta \leqslant \theta_{wp} \\ 1 & \text{for } \theta > \theta_{wp} \end{cases} \tag{6}$$

where θ_{wp} is the volumetric soil water content at wilting point ($m^3\ m^{-3}$). Accordingly, if soil moisture fell below the wilting point, evapotranspiration was stopped for that soil layer and we assumed that the evapotranspiration that could not be fulfilled (i.e. the difference between the forcing data and the modelled evapotranspiration) would be supplied by water from deeper layers (i.e. at depths greater than the maximum rooting depth). This assumption appeared reasonable given the uncertainty in describing the maximum rooting depth (i.e. using information from the literature for a single species) as well as evidence that trees can tap water from deep soil layers or even groundwater (Miller et al., 2010; Thompson et al., 2011).

3.2. Description of the HydroGeoSphere model

As a state-of-the-art integrated surface and subsurface hydrologic model, HydroGeoSphere (HGS) offers a benchmark against which to compare HydroSVS. HGS is an integrated surface and

subsurface hydrologic model that simultaneously solves for two-dimensional overland flow and three-dimensional variably saturated flow (Aquanty, 2013). Overland surface flow is simulated with the diffusion-wave approximation of the Saint-Venant equations and subsurface variably saturated flow is simulated with a modified form of Richards' equation. The equations are discretized with the control-volume finite element mode (Forsyth, 1991). The surface and subsurface domains are coupled with the dual node approach, which uses a first-order exchange coefficient between the domains. The relationship between soil water content, soil water potential and relative permeability is described using the van Genuchten (1980) model. A detailed description of equations and their numerical implementation is found in Aquanty (2013). Previous studies have successfully used HGS to simulate soil moisture and the model showed an excellent ability to capture spatio-temporal dynamics in a small catchment (Koch et al., 2016). Moreover, the model was part of an initiative for surface-subsurface model intercomparison and it successfully simulated soil saturation in a benchmark test case (Maxwell et al., 2014).

In HGS, the Kristensen and Jensen (1975) model is implemented to simulate transpiration and evaporation as a function of potential evapotranspiration and water availability at each node within the root and evaporation zones. However, in this study, eddy-covariance measurements of evapotranspiration were used as an input to the model (see Section 3.4 for a description of the boundary conditions). Similar to the HydroSVS simulations, we assumed that soil evaporation and interception were negligible and that only transpiration occurred, as described in Eq. (3). In HGS, the root distribution function $r(z)$ followed a cubic law between the surface and the maximum root depth. Since the actual relationship at each site is unknown, the transpiration reduction function $f(\theta)$ was parametrized either as a step function (Eq. (6)) or as a linear function according to:

$$f(\theta) = \begin{cases} 0 & \text{for} \quad \theta \leqslant \theta_{wp} \\ \frac{\theta - \theta_{wp}}{\theta_{fc} - \theta_{wp}} & \text{for} \quad \theta_{wp} < \theta < \theta_{fc} \\ 1 & \text{for} \quad \theta \geqslant \theta_{fc} \end{cases} \tag{7}$$

where θ_{fc} is the volumetric soil water content at field capacity ($m^3\ m^{-3}$). According to Eq. (7), if soil moisture falls below field capacity, transpiration is reduced and modelled evapotranspiration is thus smaller than the observed evapotranspiration used as forcing data. Moreover, only soil water over the root zone is available for transpiration and the HGS model cannot tap deep soil layers to feed the transpiration flux.

3.3. Model setup

HydroSVS and HGS were both set up to perform one-dimensional soil column simulations (Fig. 2). We chose to discretize the soil differently in order to reflect how each model is typically set up for operational applications. In HydroSVS, the soil column was 3-meter-deep and divided into seven soil layers at depths of 5, 10, 20, 40, 100, 200 and 300 cm. In HGS, the soil column was 1-meter-deep and the vertical grid resolution was set to 1 cm throughout the entire column. Since all soil moisture measurements were performed in the first meter from the surface, we constrained the HGS simulations to a one-meter soil column to minimize simulation times (about one hour with HGS compared to a few seconds for HydroSVS).

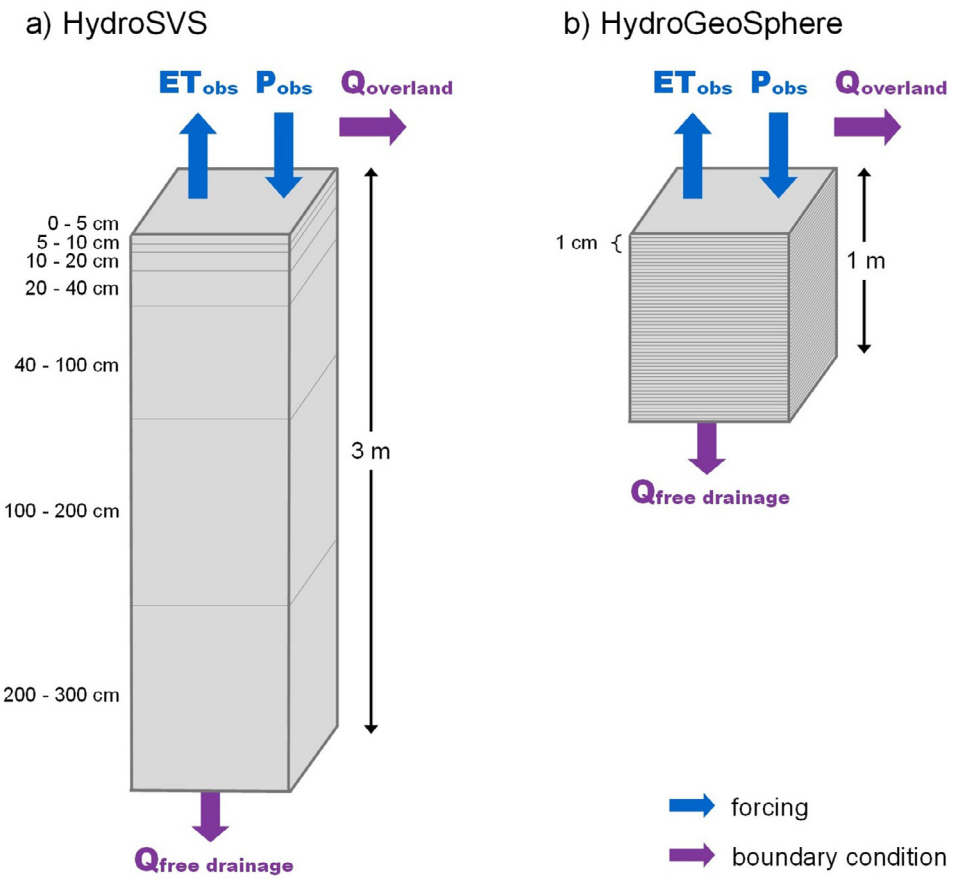

Fig. 2. Modelling framework for (a) HydroSVS and (b) HydroGeoSphere. Section 3.4 provides a detailed description of the forcings and boundary conditions.

Table 2
Soil and vegetation properties at each study site for HydroSVS and HydroGeoSphere simulations.

	US-Wkg	US-Ton	US-MRf	US-WBW
% sand – silt – clay[†]	55 – 20 – 25	48 – 42 – 10	42 – 38 – 20	28 – 60 – 12
Porosity ($m^3\ m^{-3}$)	0.44	0.56	0.44	0.38
Root depth (m)[¶]	1.2	0.7	2.2	0.6

[†] US-Wkg: Nearing et al. (2005); US-Ton: BADM from AmeriFlux database; US-MRf: Liu et al. (2013); US-WBW: Miller et al. (2007).
[¶] US-Wkg: Gibbens and Lenz (2001); US-Ton: Ichii et al. (2009); US-MRf: McMinn (1963); US-WBW: Wilson et al. (2001).

Table 3
HydroSVS and HydroGeoSphere parameters at study sites.

	HydroSVS				HydroGeoSphere			
	US-Wkg	US-Ton	US-MRf	US-WBW	US-Wkg	US-Ton	US-MRf	US-WBW
saturated hydraulic conductivity ($\times 10^{-6}$ m s^{-1})	6.40	5.00	4.05	2.47	2.81	2.93	1.06	3.62
Wilting point ($m^3\ m^{-3}$)	0.19	0.12	0.17	0.13	0.05	0.07	0.10	0.07
Field capacity ($m^3\ m^{-3}$) [†]	0.27	0.20	0.25	0.21			0.26	
Residual saturation ($m^3\ m^{-3}$)					0.01	0.02	0.06	0.05

[†] For HydroGeoSphere, the field capacity is only provided for US-MRf given a linear function is used at this site as opposed to a step function for other sites.

Table 2 lists soil and vegetation properties shared by the two models. Although soil properties are known to vary with depth, we assigned uniform properties for soil texture throughout the soil column since information at multiple depths was not available. Soil texture information was taken from the literature or metadata from the AmeriFlux database. Soil porosity was set as the maximum soil water content observed nearest to the surface at each site. Root depth was determined from data in the literature. Site-specific information on root distribution was used at US-WBW (Wilson et al., 2001) while a site-specific optimized maximum root depth from Ichii et al. (2009) was used for US-Ton. For the two other sites, maximum root depth was estimated based on the maximum root depth of the dominant species at the site, as found in the literature (Douglas fir at US-MRf in McMinn, 1963 and Lehmann lovegrass at US-Wkg in Gibbens and Lenz, 2001).

Table 3 identifies key differences between soil hydraulic properties used by the two models. Both models used the same soil texture as input data (Table 2) but differences arise since we chose to use the expressions currently implemented (HydroSVS) or most commonly used (HGS) for each model to translate texture into hydraulic properties. In HydroSVS, saturated hydraulic conductivity is computed from the soil's sand content using the expression derived by Brooks and Corey (1966). Hydraulic conductivity is assumed to exponentially decay with depth in HydroSVS (Alavi et al., 2016) while we set it up as constant in HGS simulations. For HGS simulations, we derived saturated hydraulic conductivity and residual saturation using soil texture as an input to the Rosetta model (Schaap et al., 2002). However, when the observed minimum soil water content was inferior to the Rosetta-computed residual saturation (as was the case for two sites, US-Wkg and US-Ton), residual saturation was set according to the observed minimum soil water content. In HydroSVS, the wilting point is calculated based on the clay content of the soil (Table 2) using empirical equations in Boone et al. (1999) and the field capacity is obtained using the parameterization described by Soulis et al. (2011). This method assumes that field capacity is reached through drainage of an initially saturated soil until a vertical gradient of soil moisture is established such that water potential balances out gravity. In HGS, we defined the wilting point and field capacity as the soil water content corresponding to −1.5 and −0.033 MPa, respectively, based on the water retention curve. Models also differed in the expression of the water retention curve and relative permeability. For both models, soil texture information (Table 2) was used to derive parameters describing these relationships, but different models were used: Clapp and Hornberger model in HydroSVS and van Genuchten model in HGS (see Sections 3.1 and 3.2).

3.4. Initial and boundary conditions

We defined initial subsurface conditions with soil water content measurements taken at three or more depths depending on data availability at each site. We used linear interpolation between soil moisture observations to assign initial conditions for the rest of the soil column. For initial surface conditions, we assumed a surface water depth of zero. Simulations were performed for a five-year period, with the exception of US-WBW where data were only available for 2.5 years. Precipitation and gap-filled evapotranspiration observations at a 30-min time step were used as boundary conditions for the two models. Indeed, we bypassed the internal computation of evapotranspiration within models and we rather used eddy-covariance measurements of evapotranspiration as forcing data. Gap-filling of evapotranspiration was either performed with the ReddyProc web tool (Reichstein et al., 2005; US-Wkg, US-MRf, US-WBW) or gap-filled data were already available from the CDIAC database (US-Ton). In HydroSVS, water exited the model domain as surface runoff when either surface soil moisture exceeds saturation or when the precipitation rate exceeds saturated hydraulic conductivity at the surface (hence infiltration capacity). Outflow at the bottom of the soil column occurred when soil water content exceeded field capacity and was computed with the expression developed by Soulis et al. (2011; Eq. 12). In HGS, we applied a critical depth boundary at the surface to allow overland flow to exit the model domain and we applied a unit vertical hydraulic gradient at the bottom of the soil column to allow free drainage.

3.5. Modelling performance

We evaluated the adequacy between observed and simulated values of soil water content with a series of metrics. We computed the root mean square error (RMSE) which assesses the variance of the model error. We computed the Nash-Sutcliffe efficiency (NSE) for which the optimal value is 1 and a value inferior to 0 indicates that the mean observed soil water content offers a better predictor than the model. We computed the coefficient of determination (R^2) which is the squared value of the Pearson coefficient of correlation. This metric assesses the proportion of the total variance in observations that is explained by the model. We computed the percent bias (PBIAS) which measures the average tendency of simulated

soil water content to be larger or smaller than observations. The optimal value is 0 and a positive/negative value indicates an overestimation/underestimation bias.

4. Results

Metrics describing the agreement between observed and modelled soil water content are presented in Table 4. These metrics are presented for the middle soil layers which correspond to measurement depths of 15, 20, 30 and 20 cm at US-Wkg, US-Ton, US-MRf and US-WBW respectively. It should be noted that these metrics were computed by comparing soil water content measurements at a single depth to modelled values corresponding to the average soil moisture over a certain soil depth (depth = 10 cm at US-Wkg and 20 cm at other sites).

4.1. Soil moisture modelling under a semiarid climate (US-Wkg)

At the US-Wkg site, the mean annual precipitation was 324 mm during the study period, with 2013 being the driest year (264 mm) and 2014 the wettest year (415 mm; Fig. 3a). During the study period (2010–2014), 2010 experienced an unusually wet winter, with 110 mm in the first five months of the year compared to an average of 36 mm for the other years. The performance of HydroSVS was weak at the semiarid site, as illustrated by the negative value of the Nash-Sutcliffe coefficient (NSE = −2.69; Table 4). During the dry season (January to June), soil moisture was completely depleted near the surface (0–5 cm) in the HydroSVS simulations (Fig. 3b). While a minimum of 0.02 $m^3 m^{-3}$ was observed during dry periods, HydroSVS simulated a soil water content of 0 $m^3 m^{-3}$ in four out of five years. On the other hand, the HGS simulation was able to capture the residual water content during dry periods and soil water content did not go below 0.05 $m^3 m^{-3}$ near the surface. For deeper soil layers (10–20 cm and 20–40 cm; Fig. 3c, d), soil moisture was generally overestimated in HydroSVS simulations, with a mean value of 0.21 $m^3 m^{-3}$ at 10–20 cm over the five-year period in comparison to a mean observed soil water content of 0.10 $m^3 m^{-3}$ at 15 cm for the same period (excluding the 2010/217 to 2011/365 period given the gap in observations). Indeed, the percent bias for the mid-layer was 53% (Table 4). The only exception to this overestimation was the post-2010 monsoon period when simulated soil water content fell to 0 $m^3 m^{-3}$ in the 10–20 cm layer, although observed soil water content never went below 0.1 $m^3 m^{-3}$ at a 15-cm depth. The HGS model fared much better than HydroSVS at the deeper soil layers (10–20 cm and 20–40 cm; Fig. 3c, d). HGS simulations of soil moisture captured the observed variability in soil moisture at the middle soil layer (R^2 = 0.56; Table 4), but reduced performance was observed at the bottom soil layer (R^2 = 0.40). For example, soil water content at 30 cm varied little during the 2013 monsoon period, which did not match the HGS-simulated increase in soil water content at the bottom layer (20–40 cm; Fig. 3d).

4.2. Soil moisture modelling under a hot summer Mediterranean climate (US-Ton)

At US-Ton, precipitation events were concentrated during winter months, from October to May. Winter precipitation ranged between 511 and 557 mm during the study period, with the exception of the wet winter of 2010–2011 when precipitation reached 814 mm (Fig. 4a). HydroSVS overestimated soil moisture at all soil layers (PBIAS = 41, 15 and 30% at the top, middle and bottom soil layers), although the model performed particularly well at the middle soil layer (Fig. 4c; NSE = 0.70; Table 4). At the surface layer, both models generally failed to predict soil water content above 0.45 $m^3 m^{-3}$ while the observed maximum soil water content reached 0.56 $m^3 m^{-3}$ (Fig. 4b). During dry months (June to September), HydroSVS largely overestimated soil moisture in the surface layer: the minimum simulated soil water content was 0.16 $m^3 m^{-3}$ in the 0–5 cm layer while the observed minimum fell to 0.04 $m^3 m^{-3}$ at the surface (Fig. 4b). As a result of this overestimation, soil moisture in the HydroSVS simulation never went below the wilting point (0.12 $m^3 m^{-3}$; Table 3). In the bottom soil layer, both models generally overestimated soil water content: the minimum observed value at a 50-cm depth was 0.13 $m^3 m^{-3}$ while the minimum value modelled with HydroSVS was 0.20 $m^3 m^{-3}$ and 0.17 $m^3 m^{-3}$ with HGS for the zone at depths between 40 and 100 cm (Fig. 4d).

4.3. Soil moisture modelling under a warm summer Mediterranean climate (US-MRf)

The mean annual precipitation recorded at US-MRf ranged between 964 (in 2011) and 1337 (in 2007) mm, which was considerably lower than the long-term annual average of 1820 mm (Fig. 5a). The seasonal pattern was adequately captured by the two models and both HydroSVS and HGS were able to simulate the soil moisture decline during spring and summer months when vegetation was active. In the middle and bottom soil layers, soil moisture simulated with HydroSVS closely agreed with observations

Table 4
Model performance for the simulations of half-hourly values of soil water content at the middle soil layer at each study site.

	Model	RMSE ($m^3 m^{-3}$)	NSE	R^2	PBIAS (%)
US-Wkg	HydroSVS	0.09	−2.69	0.19	53
z_{obs} = 15 cm	HydroGeoSphere	0.04	0.39	0.56	10
z_{sim} = 10–20 cm					
US-Ton	HydroSVS	0.06	0.70	0.81	15
z_{obs} = 20 cm	HydroGeoSphere	0.04	0.86	0.91	0
z_{sim} = 20–40 cm					
US-MRf	HydroSVS	0.03	0.70	0.81	−3
z_{obs} = 30 cm	HydroGeoSphere	0.04	0.60	0.84	−8
z_{sim} = 20–40 cm					
US-WBW	HydroSVS	0.06	0.26	0.81	23
z_{obs} = 20 cm	HydroGeoSphere	0.04	0.69	0.80	5
z_{sim} = 20–40 cm					

z_{obs} is the depth of soil water content measurements, z_{sim} is the depth of the simulated soil layer; RMSE is the root mean square error; NSE is the Nash-Sutcliffe efficiency; R^2 is the coefficient of determination; PBIAS is the percent bias.

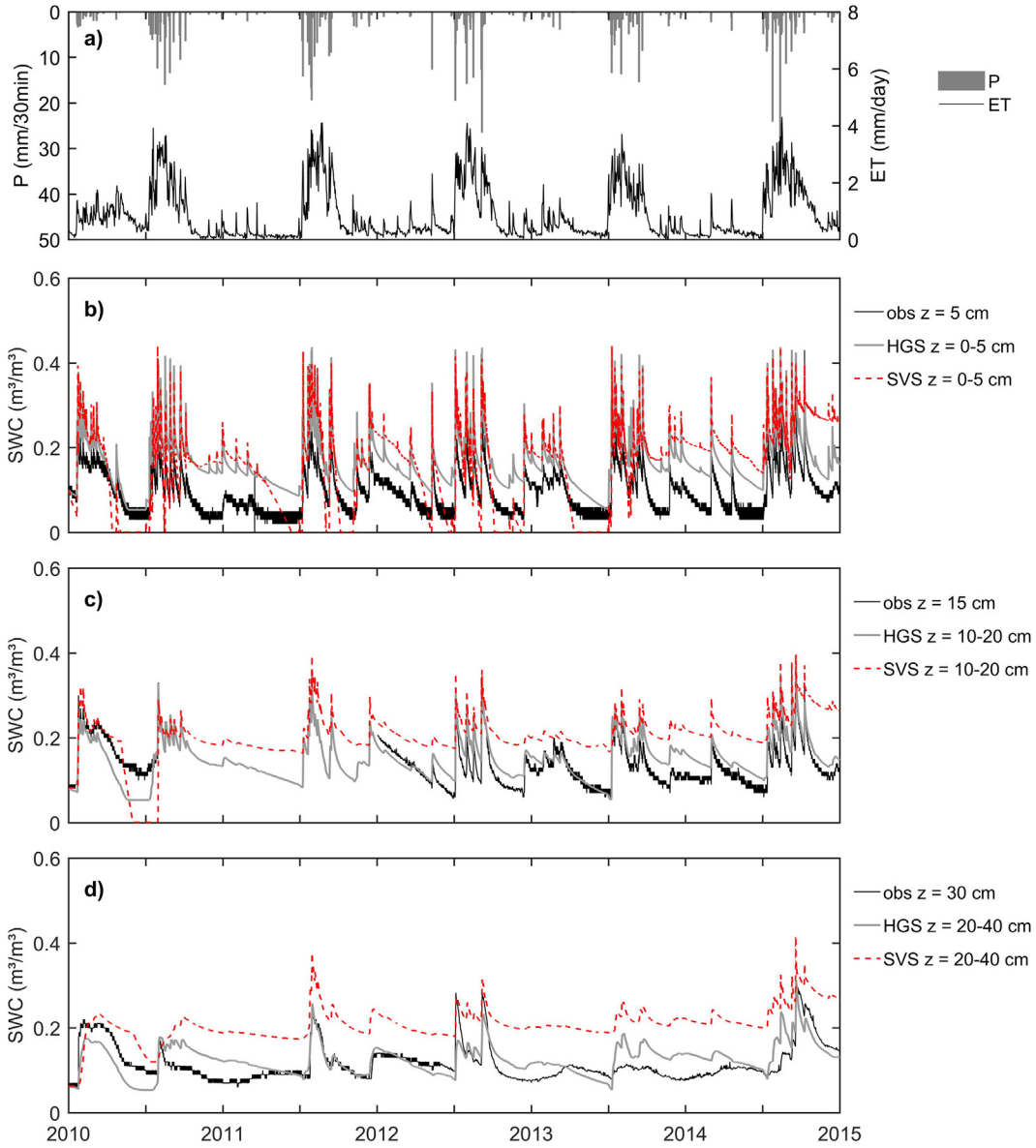

Fig. 3. Volumetric soil water content observed and modelled with HydroSVS and HGS at US-Wkg (semiarid climate; grassland vegetation).

(Fig. 5c, d). However, similar to US-Ton, soil moisture in the surface layer was overestimated by HydroSVS during drier months (June to September): the observed soil water content reached a minimum of 0.17 $m^3\ m^{-3}$ at a depth of 10 cm while the simulated minimum was 0.24 $m^3\ m^{-3}$ for the soil layer comprised between 10 and 20 cm. Accordingly, soil moisture simulated with HydroSVS never fell below the wilting point (0.17 $m^3\ m^{-3}$; Table 3). Following the rainy season (October to May), HGS adequately captured the soil moisture decline in the surface layer (Fig. 5b) but generally underestimated soil moisture during spring and summer months in the middle and bottom soil layers (Fig. 5c, d). For example, soil water content modelled with HGS at 20–40 cm dropped to 0.16 $m^3\ m^{-3}$ while the observed minimum at a depth of 30 cm remained at 0.21 $m^3\ m^{-3}$. Both models also tended to underestimate peak soil moisture during the rainy season (October to May) and often failed to simulate soil water content above 0.40 $m^3\ m^{-3}$ in the middle and bottom layers (Fig. 5c, d; PBIAS = −3% and −8% for HydroSVS and HGS; Table 4). Towards the end of the study period (second half of 2011), soil moisture appeared largely underestimated by the two models in the bottom soil layer (Fig. 5d), although we suspect that the sudden jump in soil moisture observations may be sensor-related.

4.4. Soil moisture modelling under a temperate climate (US-WBW)

Data were only available for 2.5 years at US-WBW and the study period was characterized by a wet year in 2004, with 1600 mm of precipitation, and a relatively dry year in 2005, with only 995 mm of precipitation (Fig. 6a). Both models satisfactorily captured the seasonal soil moisture pattern at US-WBW characterized by maximum soil moisture during winter months and a decrease during spring and summer months when increased vegetation activity occurred (Fig. 6). HydroSVS had difficulties capturing minimum soil moisture in the top and middle soil layers during the summer (PBIAS = 8 and 23% at the top and middle layers). For example, in the fall 2005, observed soil water content dropped to 0.05 $m^3\ m^{-3}$ at a 5-cm depth while the minimum soil water content simulated by HydroSVS and HGS was respectively 0.16 $m^3\ m^{-3}$ and 0.07 $m^3\ m^{-3}$ in the top soil layer (0–5 cm; Fig. 6a). Accordingly, soil moisture never fell below the wilting point in the HydroSVS

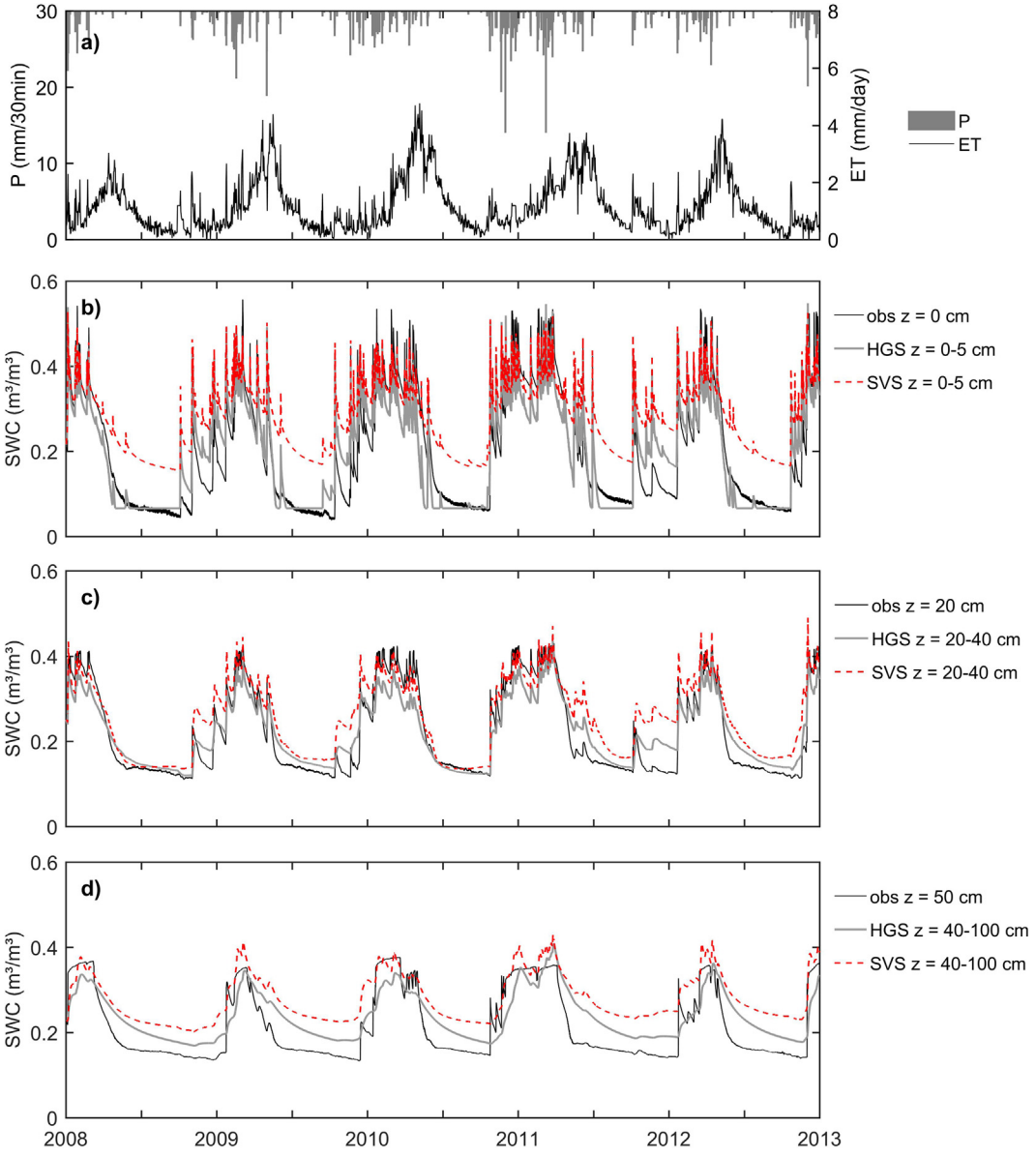

Fig. 4. Soil water content observed and modelled with HydroSVS and HGS at US-Ton (Mediterranean climate; woody savanna).

simulation ($\theta_{wp} = 0.13\ m^3\ m^{-3}$; Table 3) while it dropped slightly below the wilting point in the HGS simulation ($\theta_{wp} = 0.07\ m^3\ m^{-3}$; Table 3). Unlike HydroSVS, which adequately captured high soil water content values during the winter, HGS generally underestimated soil water content in the middle soil layer during this period. Indeed, observed soil water content generally remained above $0.25\ m^3\ m^{-3}$ at 20 cm during the winter while HGS-simulated soil water content hovered around $0.22\ m^3\ m^{-3}$ for the soil layer ranging between 20 and 40 cm (Fig. 6c). Still, the two models were able to capture the short-lived peaks in soil moisture during winter months. At the bottom soil layer (40–100 cm; Fig. 6), both models underestimated soil water content throughout the entire study period (PBIAS = −16% and −27% for HydroSVS and HGS). For example, while observed soil water content remained around $0.34\ m^3\ m^{-3}$ during winter months, simulated soil water content was generally below $0.30\ m^3\ m^{-3}$ and $0.25\ m^3\ m^{-3}$ for HydroSVS and HGS respectively. However, this underestimation could be due to a change in porosity at lower depths given that observed soil water content plateaued at lower values in surface layers ($0.28\ m^3\ m^{-3}$ at z = 5 cm and $0.26\ m^3\ m^{-3}$ at z = 20 cm).

5. Discussion

5.1. Tapping into flux tower networks to assess subsurface hydrological processes

The AmeriFlux sites have largely been used to evaluate the representation of surface processes such as evapotranspiration in land surface models (Williams et al., 2009). However, the network also offers a great opportunity to isolate and evaluate subsurface processes. Evapotranspiration introduces considerable uncertainty in hydrological modelling (Seiller and Anctil, 2016) and numerous efforts have been dedicated to improve its simulation (Courault et al., 2005; Salvucci and Gentine, 2013; Wang and Bras, 2011). The approach used in the present study provides new insight by decoupling two aspects of the evapotranspiration flux: its

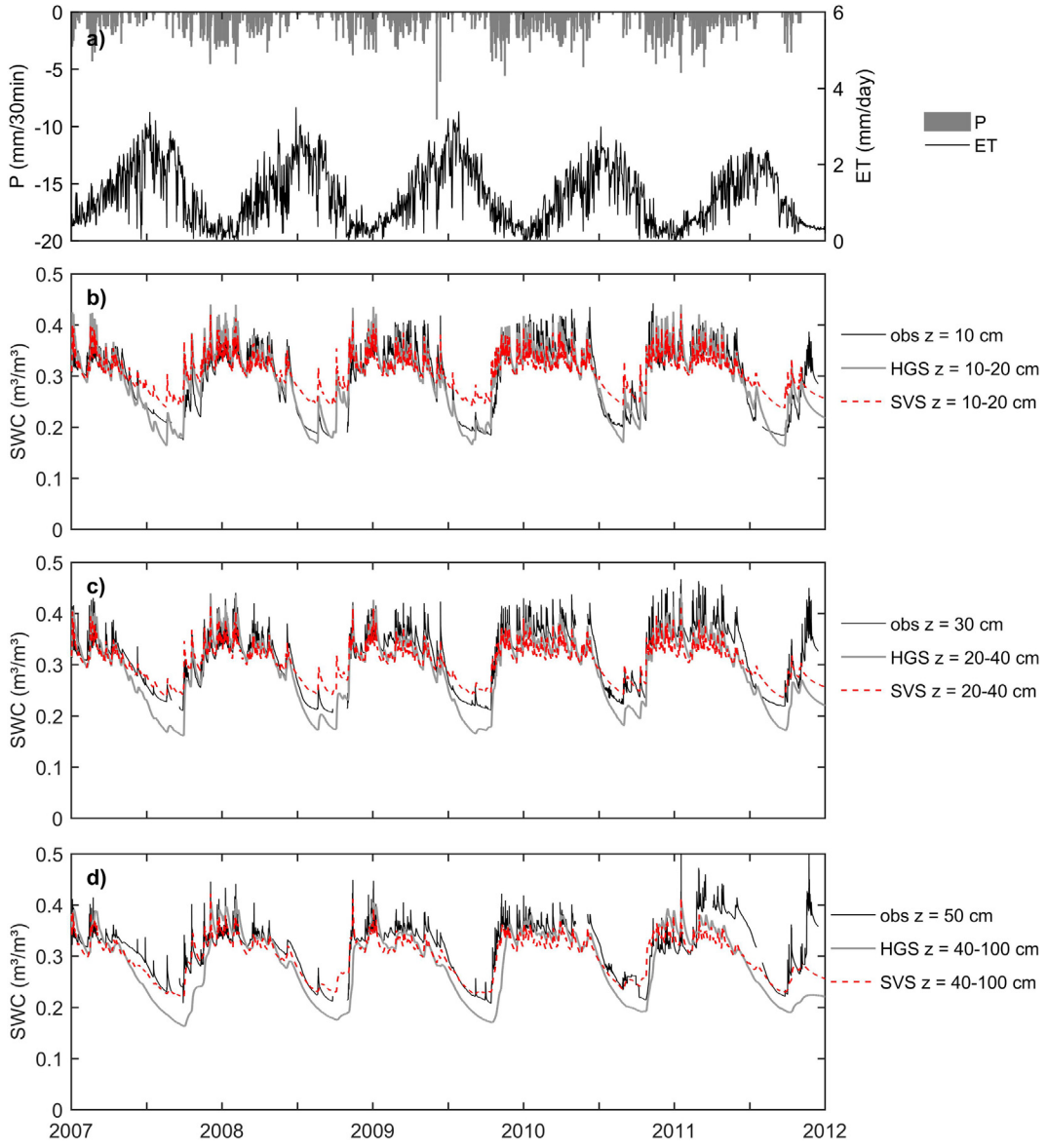

Fig. 5. Soil water content observed and modelled with HydroSVS and HGS at US-MRf (Mediterranean climate; evergreen needleleaf forest).

magnitude and its sourcing. Indeed, by providing data on the evapotranspiration magnitude, the AmeriFlux dataset allowed us to focus on the sourcing portion of this flux. While flux tower networks offer insight into the magnitude of water vapor fluxes, eddy covariance measurements also tend to underestimate available energy with a mean imbalance of about 20% on an annual time scale (Stoy et al., 2013; Wilson et al., 2002). The energy imbalance problem is particularly acute with data at a half-hourly time scale (i.e. input data used in the present study) and generally attenuates over a daily time scale (Leuning et al., 2012). This energy imbalance may translate into an underestimation of evapotranspiration (Foken, 2008) which could lead to an overestimation of soil moisture when using the observed evapotranspiration as forcing data. In the present study, no distinct pattern of under- or overestimation emerged in simulations. During periods of maximum evapotranspiration, we observed an overestimation of soil moisture in the middle soil layer in HydroSVS simulations (PBIAS between 15 and 53%, except for −3% at US-MRf; Table 4), while HGS generally performed well during these periods PBIAS between −8% and 10%; Table 4), thus suggesting that the input data were not responsible. A larger sample size would be necessary to assess if the energy imbalance of eddy covariance measurements translates into a systematic bias in soil moisture modelling using observed evapotranspiration as forcing data. An underestimation of evapotranspiration by eddy covariance measurements could also be potentially compensated by the wind-induced undercatch of precipitation by rain gauges (Sevruk, 1982). Moreover, a spatial mismatch can also arise between the location of soil moisture measurements and the footprint of flux tower observations of evapotranspiration. Indeed, evapotranspiration measurements are representative of the region upwind of the flux tower (typically within a distance of approximately 100 times the tower height) and water availability could differ from soil moisture measurements at the foot of the flux tower. Such mismatch could translate into differences between observed evapotranspiration, which is used as forcing data, and evapotranspiration actually taking place at the soil column where moisture measurements are being performed.

5.2. Soil moisture modelling under a semiarid climate

Soil moisture modelling under a semiarid climate proved challenging for HydroSVS which resulted in a negative Nash-Sutcliffe

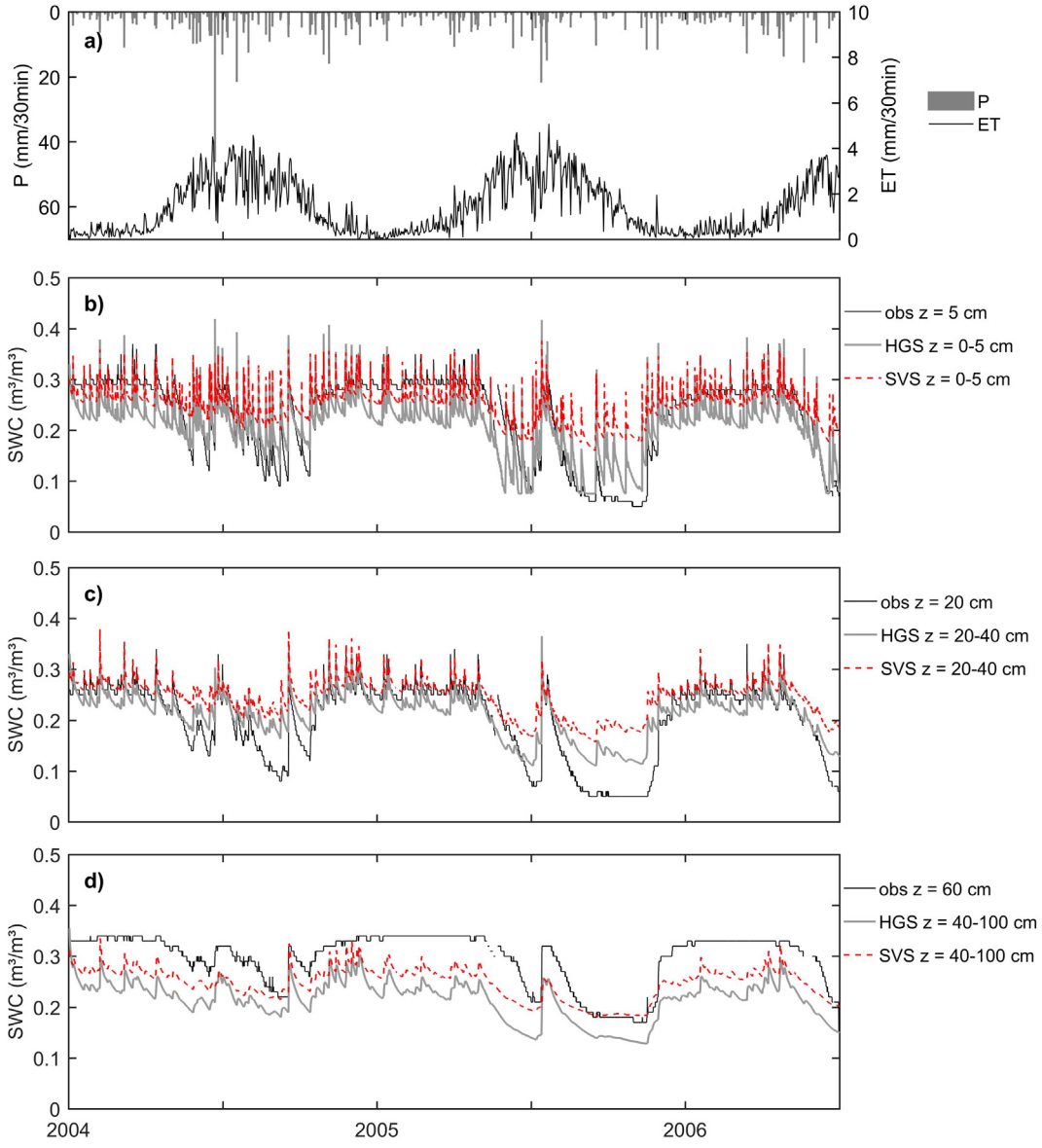

Fig. 6. Soil water content observed and modelled with HydroSVS and HGS at US-WBW (temperate climate, deciduous broadleaf forest).

coefficient (Table 4). In the HydroSVS simulation, soil moisture was underestimated and sometimes completely depleted near the surface during dry months while it was overestimated in deeper soil layers (US-Wkg; Fig. 3). Given the ability of HGS to properly simulate soil moisture at this site, the input data (soil texture) used to derive hydraulic soil properties do not appear to be a reasonable explanation of the relatively poor performance of HydroSVS. In fact, our ability to rule out this issue and raise questions about the model itself stems from our evaluation approach that not only relies on observations but also considers the comparison with another model. Reduced performance for HydroSVS could be in part explained by differences in water retention curve used by the two models. Indeed, the HGS model relied on the van Genuchten model to describe the water retention curve and this model involved an additional parameter, residual saturation, which is not part of the Clapp and Hornberger (1978) model implemented in HydroSVS. Soil moisture can thus become completely depleted in HydroSVS simulations, largely as a result of drainage since evapotranspiration will stop when soil moisture goes below the wilting point. Instead, minimum soil water content could not go below residual saturation in HGS simulations, which could explain its enhanced performance during rain-free periods. It should also be noted that residual saturation defined in HGS simulations were adjusted based on soil moisture observations at US-Wkg, which was not the case in HydroSVS simulations. Indeed, residual saturation derived using soil texture data as input the Rosetta model was 0.07 $m^3\ m^{-3}$ and instead, we set residual saturation to 0.02 $m^3\ m^{-3}$ in the HGS simulation in order to match the observed minimum soil moisture. When soil moisture observations are lacking to make such adjustments, a correction to water retention curves could also be applied to avoid overestimation of residual soil moisture under arid climates (Ciocca et al., 2014).

5.3. Soil moisture modelling under Mediterranean and temperate climates

Under Mediterranean and temperate climates, HydroSVS provided realistic soil moisture time series when observed precipitation and evapotranspiration were used as inputs. In general, HydroSVS had a performance comparable to that of the integrated

surface and subsurface hydrologic model HGS model. In fact, increased complexity did not yield better results and HydroSVS even outperformed HGS at US-MRf (NSE = 0.70 with HydroSVS compared to NSE = 0.60 with HGS; Table 4). As such, the vertical resolution in the soil column in HydroSVS appeared sufficient to capture soil moisture variability under Mediterranean and temperate climates. Moreover, simulation times for a five-year period were in the order of seconds for HydroSVS in comparison to approximately one hour with HGS. Overall, HydroSVS satisfactorily captured the time evolution of soil moisture following precipitation events and the model was able to reproduce maximum soil moisture conditions. Given the importance associated with the estimation of peak flows in hydrology, this behavior appears particularly relevant when assessing the potential of HydroSVS for hydrological prediction. Gaborit et al. (2017) demonstrated the satisfactory performance of the GEM-Hydro platform (where SVS is combined with the WATROUTE routing scheme) for streamflow prediction in tributaries of Lake Ontario, North America. These results in terms of soil moisture and streamflow modelling are promising relative to the use of land surface models in hydrology.

The performance of both models, HydroSVS and HGS, was generally best for the middle soil layer at depths between 20 and 40 cm while the weakest performance was generally found for the bottom soil layer (Figs. 4–6). The good agreement between observed and modelled values in the middle layers suggests adequate modelling of the root zone, despite the lack of information on the latter. As for the reduced modelling performance in the bottom soil layer, the fact that observations represent a point measurement at a specific depth while modelled values represent mean soil water content for a 60-cm deep layer (20 cm for US-Wkg) could explain discrepancies between observed and modelled values. Moreover, disagreement between observed and modelled values at the bottom layer could also be associated with the challenge of capturing changes in soil properties with depth. Indeed, we used soil texture information sampled at a single depth to define soil hydraulic properties although the texture is known to change throughout the soil profile. Still, a previous study by Alavi et al. (2016) found that depth-varying soil texture only had a small influence on the performance of soil moisture modelling near the surface.

For the HGS simulation at US-MRf, we parametrized the transpiration reduction function as a linear function (Eq. (7)) rather than as a step function (Eq. (6)) as was the case for all other simulations. We opted for this linear parameterization given a step function led to a large underestimation of soil moisture with HGS and the more gradual onset of water stress, as represented by the linear function, appeared better suited. Little guidance is generally offered in the literature regarding the definition of water stress points (e.g. wilting point, field capacity) and the shape of transpiration reduction functions under forested (as opposed to agricultural) settings although the formulation of these functions can have a substantial impact on water budget simulations (Ferguson et al., 2016). For example, field capacity is often used to define the upper limit of water stress conditions in models, although there is little empirical evidence that this hydrological variable, which describes drainage conditions, can be readily associated with water stress conditions for vegetation. Moreover, the shape of transpiration reduction functions is often hard-coded in models, leaving little flexibility for adjustment. However, vegetation can exhibit considerable variability in terms of transpiration reduction functions. For example, isohydric behavior in plants is associated with early stomatal closure in response to water stress, which would typically translate into steep transpiration reduction functions. On the other hand, anisohydric behavior means plants tend to maintain stomata open thus leading to a more gradual decrease in transpiration reduction functions (Verhoef and Egea, 2014). Overall, more work is needed to improve the definition of transpiration reduction functions and the proposed framework (i.e. using observed evapotranspiration as forcing data) could help find answers.

5.4. Sources of uncertainty in simulating soil moisture

Using evapotranspiration observations as a forcing, we were able to reduce uncertainty associated with the simulation of this flux for the most part (the uncertainty associated with eddy-covariance measurements of course remains), thus allowing to focus on subsurface processes and properties. First, we discuss sources of uncertainty in HydroSVS simulations that the comparison with HGS brought out. Second, we discuss sources of uncertainty associated with both models.

Both models, HydroSVS and HGS, describe unsaturated flow using Richards equation, ruling out this aspect as a source of divergence between them. Unlike many model comparison studies (Breuer and Huisman, 2009; Smith et al., 2012; Vansteenkiste et al., 2014), the present one did not seek to compare the use of conceptual reservoir scheme versus Richards equation to represent flow in an unsaturated medium. While both models use the same governing equation to describe unsaturated flow, the representation is simplified in mainly two ways in HydroSVS: flow is simulated in one dimension, as opposed to a three-dimensional simulation with HGS, and the soil column is represented with a lower vertical resolution with compartments that vary in size between 5 and 60 cm in the top meter, as opposed to a 1-cm vertical discretization in HGS. Our study was not designed to specifically assess gains in performance associated with a single- versus multidimensional of flow representation, but Koch et al. (2016) showed that a three-dimensional representation of unsaturated flow did not improve soil moisture simulation over a small catchment. As for vertical resolution, HydroSVS is particularly sensitive to the vertical root profile since it largely determined from which soil zone water uptake took place, as opposed to HGS simulations that used a very fine discretization of the soil column. As discussed in Section 5.2, HydroSVS performed relatively poorly at the semiarid site and the use of the van Genuchten model, which includes a term for residual soil moisture, appeared like a more suited choice to describe the water retention curve under a semiarid climate. Overall, HydroSVS had a slightly weaker but overall comparable performance to the more complex model HGS (with the exception of the semiarid site). Other studies have shown that simple models can perform similarly or even better than complex ones when simulating soil moisture (Orth et al., 2015; Orth and Seneviratne, 2015). Given their lower computational demand, simple models represent useful tools to sample the entire parameter space with automatic calibration, to model soil moisture when only poorly resolved input data are available, or to perform forecasts over large domains. On the other hand, complex models include an explicit and detailed description of processes which can make them better equipped to simulate changing (climate or land use) conditions.

While we have identified here a few areas of improvement for HydroSVS, it should be noted that only small gains in performance were achieved when simulating soil moisture with HGS at sites with Mediterranean and temperate climates. This illustrates the limits of increasing model complexity and points towards other aspects, such as parameter allocation (i.e. assigning values to soil and vegetation properties) to improve soil moisture simulation. In this study, automatic parameter calibration was not used and instead, we relied on observations at the AmeriFlux sites, values taken from the literature, and pedo-transfer functions (PTFs) to set soil and vegetation properties. Different PTFs were used to set soil hydraulic parameters: Clapp and Hornberger for HydroSVS

and Rosetta for HGS. The choice of PTFs can introduce considerable uncertainty and Baroni et al. (2010) found that PTFs introduced greater uncertainty in soil moisture simulations than the choice of a conceptual versus physically-based hydrological model. Still, no distinct superiority emerges in the literature among PTFs. To reduce uncertainty associated with the estimation of soil hydraulic parameters, we used soil water content observations to set porosity or adjust residual saturation parameters. This tailoring improved model performance but, given the paucity of information on soil and vegetation properties, the description of other properties had to be simplified. When setting soil hydraulic parameters, we assigned homogeneous properties over the modelling domain (except for hydraulic conductivity which varied with depth in HydroSVS simulations, see Section 3.3) even though soil properties generally vary with depth and the inclusion of this information has been shown to improve simulations (Decharme et al., 2006). Apart from soil hydraulic properties, there is considerable uncertainty regarding the definition of stress points (wilting point and field capacity) in transpiration reduction functions. Such stress points are generally set using fixed thresholds in soil water potential (−1.5 MPa and −0.033 MPa in this study). However, these soil water potential thresholds have been shown to vary between vegetation types (Emanuel et al., 2007; Miller et al., 2007). For example, wilting can be initiated at a lower threshold of water availability for vegetation in semiarid climates (−2 to −4 MPa; Baldocchi et al., 2004) and, as such, the wilting point at the semiarid site (US-Wkg) may have been overestimated, especially in the HydroSVS simulation (wilting point = 0.19 $m^3\ m^{-3}$; Table 3). Moreover, field capacity (water potential = −0.033 MPa) has largely been used to define the onset of water stress in vegetation, although research indicates that the use of this proxy may not always be appropriate (Miller et al., 2007). The vertical root profile also proves challenging to describe and, as in HGS, only the maximum rooting depth is often taken into consideration in hydrological and land surface models. While an additional parameter describes the shape of the root profile in HydroSVS ($\boldsymbol{c}$ in Eq. (5)), rarely are the data available to set it in an informed way. This is a good example where model capacity appears to have surpassed our ability to allocate values to parameters, as it often appears to be the case for subsurface properties.

5.5. Limitations

This project used one-dimensional column simulations to assess the ability of models to simulate soil moisture. This simplified representation, which assumes vertical flow only, appeared reasonable given the study sites were located on relatively flat terrain as are most sites of the AmeriFlux network. Lateral flow was not taken into consideration in this study although it can play an important role, particularly over sloped terrain. The representation of lateral flow processes has been identified as an area for improvement in land surface models (Davison et al., 2016) and HydroSVS proposes an improved parameterization of this hydrological process (Alavi et al., 2016). Further work is needed to assess the representation of this process in HydroSVS.

In this study, model fidelity was assessed by comparing observed and modelled values of volumetric soil water content. However, soil moisture exhibits substantial spatiotemporal variability. For example, the coefficient of variation of soil moisture measurements can range between 10 and 50% over a 100 m scale (Famiglietti et al., 2008; Gwak and Kim, 2017; Hang et al., 2016). Measurements at a single location, as it is the case here, cannot capture this horizontal variability in soil moisture. Additionally, uncertainty is also associated with the vertical positioning of soil moisture probes. Indeed, a precise definition of the surface can be difficult in the presence of rocks and litter and will affect our ability to compare observed and modelled values at a given depth. It should also be noted that observations are performed at a single depth, while modelled values correspond to the average soil moisture over a certain soil depth that ranged between 5 and 60 cm.

When using evapotranspiration observations as forcing data, a divergence may occur between the observed and simulated flux, if soil moisture in the root zone falls below the wilting point. As described in Section 3.1, in this case, HydroSVS was set up to tap water from deeper soil layers to fulfill the observed evapotranspiration flux. In HydroSVS simulations, soil moisture in the root zone did not go below the wilting point at the Mediterranean and temperate sites and as such, we did not encounter this issue. At the semiarid site, soil moisture in the top layers fell below the wilting point, but modelled evapotranspiration was still able to match the forcing data by taping water from lower soil compartments within the root zone. Still, a mismatch between the observed and simulated evapotranspiration flux is a limitation of the proposed approach that should be kept in mind and this disparity could be due to a misdefinition of either the wilting point or the root zone depth.

Last, this study focused exclusively on warm season hydrological processes and we selected only snow-free sites. The ability of the model to represent soil freeze-thaw processes, which have a considerable influence on soil moisture in colder climates, was not explored. To better account for these processes, a new snow module (ISBA-ES) is currently being implemented into SVS, which currently relies on a simple force-restore approach.

6. Conclusions

This study used flux-tower observations of evapotranspiration as forcing data to assess the ability of HydroSVS, the hydrological module of the SVS land surface model, to simulate soil moisture under snow-free conditions. By decoupling two aspects of evapotranspiration (i.e. its magnitude and its sourcing), this approach provides a powerful diagnostic tool regarding the representation of subsurface hydrological processes in land surface models. In this study, we compared the performance of HydroSVS to soil moisture simulations performed with HGS, a state-of-the-art integrated surface and subsurface hydrologic model, thus providing important context relative to the trade-off between model fidelity and complexity. Overall, HydroSVS provided a realistic simulation of soil moisture under Mediterranean and temperature climates (sites US-Ton, US-MRf, US-WBW) and, as illustrated by HGS simulations, increased model complexity yielded only minor improvements in terms of soil moisture modelling. As such, this study provides a strong argument regarding the potential of SVS for hydrological applications. Under a semiarid climate (site US-Wkg), soil moisture modelling proved challenging for HydroSVS. The successful simulation of soil moisture with HGS suggests that certain features, such as the inclusion of residual saturation when defining water retention curves, can be beneficial when simulating soil moisture under a semiarid climate.

Acknowledgements

This research was supported by the Natural Sciences and Engineering Research Council of Canada (grant RGPIN/04892-2015). Funding for AmeriFlux data resources was provided by the U.S. Department of Energy's Office of Science. We thank the primary investigators of the AmeriFlux sites that made this research possible by making their data available: Russel Scott (US-Wkg), Dennis Baldocchi (US-Ton), Bev Law (US-MRf) and Tilden Meyers (US-WBW). We also thank Dr. Rene Orth and an anonymous reviewer whose suggestions helped improve the manuscript.

References

Alavi, N., Bélair, S., Fortin, V., Zhang, S., Husain, S.Z., Carrera, M.L., Abrahamowicz, M., 2016. Warm season evaluation of soil moisture prediction in the soil, vegetation and snow (SVS) scheme. J. Hydrometeorol. 17, 2315–2332. https://doi.org/10.1175/JHM-D-15-0189.1.

Aquanty, 2013. HydroGeoSphere User Manual. Release 1.0. Aquanty Inc., Waterloo, Ontario, Canada.

Baldocchi, D.D., Falge, E., Gu, L., Olson, R., Hollinger, D., Running, S., Anthoni, P., Bernhofer, C., Davis, K., Evans, R., Fuentes, J., Goldstein, A., Katul, G., Law, B., Lee, X., Malhi, Y., Meyers, T., Munger, W., Oechel, W., Paw, K.T.U., Pilegaard, K., Schmid, H.P., Valentini, R., Verma, S., Vesala, T., Wilson, K., Wofsy, S., 2001. FLUXNET : A new tool to study the temporal and spatial variability of ecosystem-scale carbon dioxide, water vapor, and energy flux densities. Bull. Am. Meteorol. Soc. 82, 2415–2434.

Baldocchi, D., 2016. AmeriFlux US-Ton Tonzi Ranch. https://doi.org/10.17190/AMF/1245971.

Baldocchi, D.D., Xu, L., Kiang, N., 2004. How plant functional-type, weather, seasonal drought, and soil physical properties alter water and energy fluxes of an oak-grass savanna and an annual grassland. Agric. For. Meteorol. 123, 13–39. https://doi.org/10.1016/j.agrformet.2003.11.006.

Baroni, G., Facchi, A., Gandolfi, C., Ortuani, B., Horeschi, D., Van Dam, J.C., 2010. Uncertainty in the determination of soil hydraulic parameters and its influence on the performance of two hydrological models of different complexity. Hydrol. Earth Syst. Sci 14, 251–270. https://doi.org/10.5194/hess-14-251-2010.

Bélair, S., Brown, R., Mailhot, J., Bilodeau, B., Crevier, L.-P., 2003. Operational implementation of the ISBA land surface scheme in the Canadian regional weather forecast model. Part I: warm season results. J. Hydrometeorol. 4, 371–386.

Boone, A., Calvet, J.-C., Noilhan, J., 1999. Inclusion of a third soil layer in a land surface scheme using the force–restore method. J. Appl. Meteorol. 38, 1611–1630.

Breuer, L., Huisman, J.A., 2009. Assessing the impact of land use change on hydrology by ensemble modeling (LUCHEM). Adv. Water Resour. 32, 127–128. https://doi.org/10.1016/j.advwatres.2008.10.010.

Brooks, R.H., Corey, A.T., 1966. Properties of porous media affecting fluid flow. J. Irrig. Drain. Div. 92, 61–88.

Ciocca, F., Lunati, I., Parlange, M.B., 2014. Effects of the water retention curve on evaporation from arid soils. Geophys. Res. Lett. 41, 3110–3116. https://doi.org/10.1002/2014GL059827.

Clapp, R.B., Hornberger, G.M., 1978. Empirical equations for some soil hydraulic properties. Water Resour. Res. 14, 601–604.

Clark, M.P., Fan, Y., Lawrence, D.M., Adam, J.C., Bolster, D., Gochis, D.J., Hooper, R.P., Kumar, M., Leung, L.R., Mackay, D.S., Maxwell, R.M., Shen, C., Swenson, S.C., Zeng, X., 2015a. Improving the representation of hydrologic processes in Earth system models. Water Resour. Res. 51, 5929–5956. https://doi.org/10.1002/2015WR017096.

Clark, M.P., Nijssen, B., Lundquist, J.D., Kavetski, D., Rupp, D.E., Woodsa, R., Freer, J.E., Gutmann, E.D., Wood, A.W., Brekke, L.D., Arnold, J.R., Gochis, D.J., Rasmussen, R. M., 2015b. A unified approach for process-based hydrologic modeling: 1 Modeling concept. Water Resour. Res. 51, 2498–2514. https://doi.org/10.1002/2015WR017200.A.

Courault, D., Seguin, B., Olioso, A., 2005. Review on estimation of evapotranspiration from remote sensing data: from empirical to numerical modeling approaches. Irrig. Drain. Syst. 19, 223–249.

Davison, B., Pietroniro, A., Fortin, V., Leconte, R., Mamo, M., Yau, M., 2016. What is missing from the prescription of hydrology for land surface schemes? J. Hydrometeorol. 17, 2013–2039. https://doi.org/10.1175/JHM-D-15-0172.1.

Decharme, B., Douville, H., Boone, A., Habets, F., Noilhan, J., 2006. Impact of an exponential profile of saturated hydraulic conductivity within the ISBA LSM: simulations over the Rhône Basin. J. Hydrometeorol. 7, 61–80. https://doi.org/10.1175/JHM469.1.

Emanuel, R.E., D'Odorico, P., Epstein, H.E., 2007. A dynamic soil water threshold for vegetation water stress derived from stomatal conductance models. Water Resour. Res. 43, 1–13. https://doi.org/10.1029/2005WR004831.

Famiglietti, J.S., Ryu, D., Berg, A.A., Rodell, M., Jackson, T.J., 2008. Field observations of soil moisture variability across scales. Water Resour. Res. 44, W01423. https://doi.org/10.1029/2006WR005804.

Ferguson, I.M., Jefferson, J.L., Maxwell, R.M., Kollet, S.J., 2016. Effects of root water uptake formulation on simulated water and energy budgets at local and basin scales. Environ. Earth Sci. 75, 316. https://doi.org/10.1007/s12665-015-5041-z.

Foken, T., 2008. The energy balance closure problem: an overview. Ecol. Appl. 18, 1351–1367. https://doi.org/10.1890/06-0922.1.

Forsyth, P.A., 1991. A control volume finite element approach to NAPL groundwater contamination. SIAM J. Sci. Stat. Comput. 12, 1029–1057.

Gaborit, É., Fortin, V., Xu, X., Seglenieks, F., Tolson, B., Fry, L.M., Hunter, T., Anctil, F., Gronewold, A.D., 2017. A hydrological prediction system based on the SVS land-surface scheme: efficient calibration of GEM-Hydro for streamflow simulation over the Lake Ontario basin. Hydrol. Earth Syst. Sci. 21, 4825–4839. https://doi.org/10.5194/hess-21-4825-2017.

Gibbens, R., Lenz, J., 2001. Root system of some chihuhuan desert plants. J. Arid Environ. 49, 221–263.

Gwak, Y., Kim, S., 2017. Factors affecting soil moisture spatial variability for a humid forest hillslope. Hydrol. Process. 31, 431–445. https://doi.org/10.1002/hyp.11039.

Hang, C., Nadeau, D.F., Jensen, D.D., Hoch, S.W., Pardyjak, E.R., 2016. Playa soil moisture and evaporation dynamics during the MATERHORN field program. Boundary-Layer Meteorol. 159, 521–538. https://doi.org/10.1007/s10546-015-0058-0.

Henderson-Sellers, A., Pitman, A.J., Love, P.K., Irannejad, P., Chen, T.H., 1995. The project for intercomparison of land surface parameterization schemes (PILPS): phases 2 and 3. Bull. Am. Meteorol. Soc. 76, 489–503.

Henderson-Sellers, A., Yang, Z.-L., Dickinson, R.E., 1993. The project for intercomparison of land-surface parameterization schemes. Bull. Am. Meteorol. Soc. 74, 1335–1349.

Husain, S.Z., Alavi, N., Bélair, S., Carrera, M., Zhang, S., Fortin, V., Abrahamowicz, M., Gauthier, N., 2016. The multi-budget soil, vegetation, and Snow (SVS) scheme for land surface parameterization: offline warm season evaluation. J. Hydrometeorol. 17, 2293–2313. https://doi.org/10.1175/JHM-D-15-0228.1.

Ichii, K., Wang, W., Hashimoto, H., Yang, F., Votava, P., Michaelis, A.R., Nemani, R.R., 2009. Refinement of rooting depths using satellite-based evapotranspiration seasonality for ecosystem modeling in California. Agric. For. Meteorol. 149, 1907–1918. https://doi.org/10.1016/j.agrformet.2009.06.019.

Keefer, T.O., Moran, M.S., Paige, G.B., 2008. Long-term precipitation database, Walnut Gulch experimental watershed, Arizona, United States. Water Resour. Res. 44, W05S07. https://doi.org/10.1029/2006WR005702.

Koch, J., Cornelissen, T., Fang, Z., Bogena, H., Diekkrüger, B., Kollet, S., Stisen, S., 2016. Inter-comparison of three distributed hydrological models with respect to seasonal variability of soil moisture patterns at a small forested catchment. J. Hydrol. 533, 234–249. https://doi.org/10.1016/j.jhydrol.2015.12.002.

Kristensen, K.J., Jensen, S.E., 1975. A model for estimating actual evapotranspiration from potential evapotranspiration. Nord. Hydrol. 6, 170–188. https://doi.org/10.2166/nh.1975.012.

Kwon, H., Law, B.E., Thomas, C.K., Johnson, B.G., 2017. The influence of hydrological variability on inherent water use efficiency in forests of contrasting composition, age, and precipitation regimes in the Pacific Northwest. Agric. For. Meteorol. 249, 488–500. https://doi.org/10.1016/j.agrformet.2017.08.006.

Law, B., 2016. AmeriFlux US-MRf Mary's River (Fir) site.https://doi.org/10.17190/AMF/1246049.

Leuning, R., van Gorsel, E., Massman, W.J., Isaac, P.R., 2012. Reflections on the surface energy imbalance problem. Agric. For. Meteorol. 156, 65–74. https://doi.org/10.1016/j.agrformet.2011.12.002.

Liu, S., Wei, Y., Post, W.M., Cook, R.B., Schaefer, K., Thornton, M.M., 2013. The unified north american soil map and its implication on the soil organic carbon stock in north america. Biogeosciences 10, 2915–2930. https://doi.org/10.5194/bg-10-2915-2013.

Maxwell, R.M., Chow, F.K., Kollet, S.J., 2007. The groundwater-land-surface-atmosphere connection: soil moisture effects on the atmospheric boundary layer in fully-coupled simulations. Adv. Water Resour. 30, 2447–2466. https://doi.org/10.1016/j.advwatres.2007.05.018.

Maxwell, R.M., Putti, M., Meyerhoff, S., Delfs, J., Ferguson, I.M., Ivanov, V., Kim, J., Kolditz, O., Kollet, S.J., Kumar, M., Lopez, S., Niu, J., Paniconi, C., Park, Y., Phanikumar, M.S., Shen, C., Sudicky, E.A., Sulis, M., 2014. Surface-subsurface model intercomparison: a first set of benchmark results to diagnose integrated hydrology and feedbacks. Water Resour. Res. 50, 1531–1549. https://doi.org/10.1002/2013WR013725.

McMinn, R., 1963. Characteristics of douglas-fir root systems. Can. J. Bot. 41, 105–122.

Meyers, T., 2016. AmeriFlux US-WBW Walker Branch Watershed. https://doi.org/10.17190/AMF/1246109.

Miller, G.R., Baldocchi, D.D., Law, B.E., Meyers, T., 2007. An analysis of soil moisture dynamics using multi-year data from a network of micrometeorological observation sites. Adv. Water Resour. 30, 1065–1081. https://doi.org/10.1016/j.advwatres.2006.10.002.

Miller, G.R., Chen, X., Rubin, Y., Ma, S., Baldocchi, D.D., 2010. Groundwater uptake by woody vegetation in a semiarid oak savanna. Water Resour. Res. 46, W10503. https://doi.org/10.1029/2009WR008902.

Moran, M.S., Scott, R.L., Hamerlynck, E.P., Green, K.N., Emmerich, W.E., Holifield Collins, C.D., 2009a. Soil evaporation response to Lehmann lovegrass (Eragrostis lehmanniana) invasion in a semiarid watershed. Agric. For. Meteorol. 149, 2133–2142. https://doi.org/10.1016/j.agrformet.2009.03.018.

Moran, M.S., Scott, R.L., Keefer, T.O., Emmerich, W.E., Hernandez, M., Nearing, G.S., Paige, G.B., Cosh, M.H., O'Neill, P.E., 2009b. Partitioning evapotranspiration in semiarid grassland and shrubland ecosystems using time series of soil surface temperature. Agric. For. Meteorol. 149, 59–72. https://doi.org/10.1016/j.agrformet.2008.07.004.

Nearing, M.A., Kimoto, A., Nichols, M.H., Ritchie, J.C., 2005. Spatial patterns of soil erosion and deposition in two small, semiarid watersheds. J. Geophys. Res. 110, F04020. https://doi.org/10.1029/2005JF000290.

Orth, R., Seneviratne, S.I., 2015. Introduction of a simple-model-based land surface dataset for Europe. Environ. Res. Lett. 10, 44012. https://doi.org/10.1088/1748-9326/10/4/044012.

Orth, R., Staudinger, M., Seneviratne, S.I., Seibert, J., Zappa, M., 2015. Does model performance improve with complexity? A case study with three hydrological models. J. Hydrol. 523, 147–159. https://doi.org/10.1016/j.jhydrol.2015.01.044.

Reichstein, M., Falge, E., Baldocchi, D., Papale, D., Aubinet, M., Berbigier, P., Bernhofer, C., Buchmann, N., Gilmanov, T., Granier, A., Grünwald, T., Havrankova, K., Ilvesniemi, H., Janous, D., Knohl, A., Laurila, T., Lohila, A., Loustau, D., Matteucci, G., Meyers, T., Miglietta, F., Ourcival, J.M., Pumpanen, J., Rambal, S., Rotenberg, E., Sanz, M., Tenhunen, J., Seufert, G., Vaccari, F., Vesala, T., Yakir, D., Valentini, R.,

2005. On the separation of net ecosystem exchange into assimilation and ecosystem respiration: Review and improved algorithm. Glob. Chang. Biol. 11, 1424–1439. https://doi.org/10.1111/j.1365-2486.2005.001002.x.

Salvucci, G.D., Gentine, P., 2013. Emergent relation between surface vapor conductance and relative humidity profiles yields evaporation rates from weather data. Proc. Natl. Acad. Sci. U.S.A. 110, 6287–6291. https://doi.org/10.1073/pnas.1215844110.

Schaap, M.G., Leij, F.J., Van Gencuhten, M.T., 2002. ROSETTA: a computer program for estimating soil hydraulic parameters with hierarchical pedotransfer functions. J. Hydrol. 251, 163–176.

Schenk, H.J., Jackson, R.B., 2003. Global distribution of root profiles in terrestrial ecosystems. Oak Ridge National Laboratory Distributed Active Archive Center, Oak Ridge, Tennessee, United States. doi: 10.3334/ORNLDAAC/660.

Scott, R.L. 2016. AmeriFlux US-Wkg Walnut Gulch Kendall Grassland. https://doi.org/10.17190/AMF/1246112.

Scott, R.L., Hamerlynck, E.P., Jenerette, G.D., Moran, M.S., Barron-Gafford, G.A., 2010. Carbon dioxide exchange in a semidesert grassland through drought-induced vegetation change. J. Geophys. Res. 115, G03026. https://doi.org/10.1029/2010JG001348.

Seiller, G., Anctil, F., 2016. How do potential evapotranspiration formulas influence hydrological projections? Hydrol. Sci. J. 61, 2249–2266. https://doi.org/10.1080/02626667.2015.1100302.

Seneviratne, S.I., Corti, T., Davin, E.L., Hirschi, M., Jaeger, E.B., Lehner, I., Orlowsky, B., Teuling, A.J., 2010. Investigating soil moisture-climate interactions in a changing climate: a review. Earth-Sci. Rev. 99, 125–161. https://doi.org/10.1016/j.earscirev.2010.02.004.

B. Sevruk, B., 1982. Methods of correction for systematic error in point precipitation measurement for operational use. World Meteorological Organization Operational Hydrology Report no. 21, Geneva, Switzerland.

Smith, M., Koren, V., Zhang, Z., Zhang, Y., Reed, S., Cui, Z., Moreda, F., Cosgrove, B., Mizukami, N., Anderson, E., 2012. DMIP 2 Participants, Results of the DMIP 2 Oklahoma experiments. J. Hydrol. 418–419, 17–48.

Soulis, E.D., Craig, J.R., Fortin, V., Liu, G., 2011. A simple expression for the bulk field capacity of a sloping soil horizon. Hydrol. Process. 25, 112–116. https://doi.org/10.1002/hyp.7827.

Soulis, E.D., Snelgrove, K.R., Kouwen, N., Seglenieks, F., Verseghy, D.L., 2000. Towards closing the vertical water balance in Canadian atmospheric models: coupling of the land surface scheme class with the distributed hydrological model WATFLOOD. Atmos. Ocean 38, 251–269. https://doi.org/10.1080/07055900.2000.9649648.

Stoy, P.C., Mauder, M., Foken, T., Marcolla, B., Boegh, E., Ibrom, A., Arain, M.A., Arneth, A., Aurela, M., Bernhofer, C., Cescatti, A., Dellwik, E., Duce, P., Gianelle, D., van Gorsel, E., Kiely, G., Knohl, A., Margolis, H., Mccaughey, H., Merbold, L., Montagnani, L., Papale, D., Reichstein, M., Saunders, M., Serrano-Ortiz, P., Sottocornola, M., Spano, D., Vaccari, F., Varlagin, A., 2013. A data-driven analysis of energy balance closure across FLUXNET research sites: the role of landscape scale heterogeneity. Agric. For. Meteorol. 171–172, 137–152. https://doi.org/10.1016/j.agrformet.2012.11.004.

Thompson, S.E., Harman, C.J., Konings, A.G., Sivapalan, M., Neal, A., Troch, P.A., 2011. Comparative hydrology across AmeriFlux sites: the variable roles of climate, vegetation, and groundwater. Water Resour. Res. 47, W00J07. https://doi.org/10.1029/2010WR009797.

Van Den Hurk, B., Best, M., Dirmeyer, P., Pitman, A., Polcher, J., Santanello, J., 2011. Acceleration of land surface model development over a decade of GLASS. Bull. Am. Meteorol. Soc. 92, 1593–1600. https://doi.org/10.1175/BAMS-D-11-00007.1.

van Genuchten, M.T., 1980. A closed-form equation for predicting hydraulic conductivity of unsaturated soils. Soil Sci. Soc. Am. J. 44, 892–898.

Vansteenkiste, T., Tavakoli, M., Van Steenbergen, N., De Smedt, F., Batelaan, O., Pereira, F., Willems, P., 2014. Intercomparison of five lumped and distributed models for catchment runoff and extreme flow simulation. J. Hydrol. 511, 335–349. https://doi.org/10.1016/j.jhydrol.2014.01.050.

Verhoef, A., Egea, G., 2014. Modeling plant transpiration under limited soil water: comparison of different plant and soil hydraulic parameterizations and preliminary implications for their use in land surface models. Agric. For. Meteorol. 191, 22–32. https://doi.org/10.1016/j.agrformet.2014.02.009.

Wang, J., Bras, R.L., 2011. A model of evapotranspiration based on the theory of maximum entropy production. Water Resour. Res. 47, W03521. https://doi.org/10.1029/2010WR009392.

Williams, M., Richardson, A.D., Reichstein, M., Stoy, P.C., Peylin, P., Verbeeck, H., Carvalhais, N., Jung, M., Hollinger, D.Y., Kattge, J., Leuning, R., Luo, Y., Tomelleri, E., Trudinger, C., Wang, Y.-P., 2009. Improving land surface models with FLUXNET data. Biogeosciences 6, 1341–1359. https://doi.org/10.5194/bg-6-1341-2009.

Wilson, K., Goldstein, A., Falge, E., Aubinet, M., Baldocchi, D., Berbigier, P., Bernhofer, C., Ceulemans, R., Dolman, H., Field, C., Grelle, A., Ibrom, A., Law, B.E., Kowalski, A., Meyers, T., Moncrieff, J., Monson, R., Oechel, W., Tenhunen, J., Valentini, R., Verma, S., 2002. Energy balance closure at FLUXNET sites. Agric. For. Meteorol. 113, 223–243. https://doi.org/10.1016/S0168-1923(02)00109-0.

Wilson, K.B., Hanson, P.J., Mulholland, P.J., Baldocchi, D.D., Wullschleger, S.D., 2001. A comparison of methods for determining forest evapotranspiration and its components: sap-flow, soil water budget, eddy covariance and catchment water balance. Agric. For. Meteorol. 106, 153–168.

Zabel, F., Mauser, W., 2013. 2-way coupling the hydrological land surface model PROMET with the regional climate model MM5. Hydrol. Earth Syst. Sci. 17, 1705–1714. https://doi.org/10.5194/hess-17-1705-2013.